Crystallization and Spherulitic Growth Kinetics of Poly(trimethylene terephthalate)/Polycarbonate Blends

Ez El Shafee,[1] Halla F. Naguib,[1] Longfei Li,[2] Shichun Jiang,[2] Lijia An[2]
[1] *Department of Chemistry, Faculty of Science, Cairo University, Giza 12613, Egypt*

[2] *State Key Laboratory of Polymer Physics and Chemistry, Changchun Institute of Applied Chemistry, Chinese Academy of Sciences, Changchun 130022, China*

The macroscopic and microscopic melt-crystallization kinetics of poly(trimethylene terphthalate) (PTT)/polycarbonate (PC) blends have been measured by differential scanning calorimetry (DSC), and optical microscopy (OM). The results are analyzed in terms of the Avrami equation and the Hoffman–Lauritzen crystallization theory (HL model). Blending with PC did not change the crystallization mechanism of PTT, but reduced the crystallization rate compared with that of neat PTT at the same crystallization temperature. The crystallization rate decreased with increasing crystallization temperature. The spherulitic morphology of PTT was influenced apparently by the crystallization temperature and by the addition of PC. X-ray diffraction shows no change in the unit cell dimension of PTT was observed after blending. Through the HL theory, the classical regime II→III transition was detected for the neat PTT and the blends. The nucleation parameter (K_g), the fold-surface free energy (σ_e), and the work of chain folding (q) were calculated. Blending with PC decreased all the aforementioned parameters compared with those of neat PTT. POLYM. ENG. SCI., 50:1036–1046, 2010. © 2010 Society of Plastics Engineers

INTRODUCTION

Polymer blends and composites is a rapidly growing field in polymer science and have attracted a lot of attention in both the academic and industrial communities. The fact that new materials can be developed with good properties in relatively less time and with a minimum investment has encouraged the blending of polymers. Blending of aromatic engineering polymers have been particularly interesting, because excellent properties have been observed even when the blends are immiscible [1, 2]. The good interfacial adhesion because of the interaction between the aromatic rings of these polymers may be one of the reasons for the observed behavior.

Correspondence to: Ez El Shafee; e-mail: elshafee@chem-sci.cu.edu.eg
DOI 10.1002/pen.21489
Published online in Wiley InterScience (www.interscience.wiley.com).

Poly(trimethylene terephthalate) (PTT) is a recently developed polyester that is thought to be increasingly used because it combines the good chemical resistance typical of polyesters with a resilience and elasticity similar to that of nylon 6,6. Its structure and properties are intermediate between those of poly(ethylene terphthalate) (PET) and poly(butylene terephthalate) (PBT) [3, 4].

However, the low heat distortion temperature, low melt viscosity, poor optical properties, and pronounced brittleness of unreinforced PTT at low temperature have restricted its use as a desirable engineering plastic. Some of these deficiencies could be improved by developing PTT composites or blends with suitable polymers in which it retains its excellent properties. PTT blends are expected to possess a wide range of features that will broaden the applications of the homo-polymer. Recently, a considerable amount of research work pertinent to PTT blends was reported [5–12].

Binary blends of PTT with polycarbonate (PC) are of commercial interest because of their potential in combination. Both polymers are polyester and can undergo chemical reactions at high temperatures in the solid state and in the melt, like alcoholysis or direct ester interchange, which can largely affect miscibility of the components and in some cases induce dramatic worsening of materials properties. Consequently, PTT/PC blends have been the subject of attention in the last few years. The phase structure [13–16]. ester-interchange reactions [17–19], and crystalline behavior [14, 16, 20–22] of PTT/PC blends have been studied. The blends were shown to be partially miscible [13–16] with different miscibility levels [13–19] probably because of the different interchange reaction level attained [16–19]. The progressive development of interchange reactions gives rise [20–22] to the homogenization of the blends and eventually leads to single phase materials. PC hinders PTT crystallization in the blends [17] decreasing drastically the level of crystallinity [20–22] by means of interchange reactions, that decrease the crystallizable segment length of PTT [21, 22].

Chemical exchange reactions and physical blend miscibility in mixtures of polyesters above melt temperature can be quite confusing and must be dealt with carefully, especially in temperature ranges, where possible exchange reactions may be involved. Guo and Brittain [23] have argued and questioned on correctness of the statements that trans-reaction is a pre-requisite for forming a single phase system for polyester blends. Depending on the chemical structures, some blends of polyesters can indeed be miscible without any trans-reactions. For example, the three aryl polyesters of PET, PTT, and PBT, form miscible ternary blends without any trans-reactions [24], while in other blends, trans-reactions may be necessary to bring in a single-phase [25].

Blends of PTT with PC, obtained with no detectable chemical reactions between the functional groups of the components, have been recently investigated by differential scanning calorimetry (DSC) and dielectric relaxation spectroscopy (DRS) [26]. The blend showed a single, composition-dependent glass transition temperature (T_g), suggesting that the melt-blended PTT/PC may be superficially or seemingly "miscible" according to the blend's T_g criterion. From the DSC measurement, the cold crystallization peak temperature increased, while the melting peak temperature decreased with increasing PC content.

To complete the study on the PTT/PC blends, the crystallization kinetics of the blends was investigated as a function of crystallization temperature and composition since the bulk physical properties are determined not only by miscibility (or compatibility) of the components, but also depend to a large extent on their crystalline superstructure and morphology. The addition of a second, amorphous polymeric component affects the properties of the crystalline phase of the crystallizable component, including the overall crystallinity, the crystal morphology, the dimensions of crystallites and their aggregates. Hence A complete understanding of the crystallization kinetics of semicrystalline polymer blend is essential for controlling the processing conditions and consequently the utility of materials for a given application.

EXPERIMENTAL

Materials and Blend Preparation

PTT (CORTERRA^{TM} PTT 200) polymer in the form of pellets was obtained from Shell Chemical Company. The intrinsic viscosity of the PTT at 25°C in a 60/40 mixture of phenol and tetrachloroethane was 0.9 dlg^{-1}. PC (Makrolon 1805), with MFI of 6.5 g/10 min^{-1} (ASTM D1238), was kindly supplied by Bayer. Both polymers were dried overnight in a vacuum oven at 120°C, to remove any volatiles which could cause air bubbles upon heating. The neat polymers were first ground into fine powders. This manipulation was made to ensure that thorough melt mixing could be complete within the shortest time possible. A laboratory mixing molder (ATLAS, USA) with a small mixing chamber (ca. 2 g capacity) was used to prepare the blends at 260°C and at 60 rpm under the protection of nitrogen flow. The duration time of the blending were kept as short as possible to avoid the possibility of transesterification.

Calorimetric Measurements

The isothermal crystallization behavior of PPT was investigated by using a Perkin–Elmer DSC7 calorimeter. The thermal response of the instrument was calibrated from the enthalpy of fusion of a known mass of indium (99.999% pure). The temperature scale of the calorimeter was calibrated using the melting points of indium, tin and lead. Plots of actual against experimental melting points were linear and used to calibrate the calorimeter temperature directly after correction for thermal lag by extrapolation to zero heating rate.

Samples (ca. 4–6 mg) were sealed in aluminum pans, and an empty pan was used as a reference. The samples were held in the melt at 20°C above the peak melting point of the evaluated material for period of time 3 min to erase all previous crystalline history, and then rapidly cooled by liquid nitrogen to the predetermined crystallization temperature T_c. The T_c range was chosen such that the crystallization times were no longer than 60 min. Experiments were performed to ensure that the samples did not crystallize during cooling to T_c by immediately heating the samples when the temperature reached the desired T_c; if any melting occurred, then it was concluded that the crystallization took place during cooling and the isothermal experiment was not performed at that T_c. This procedure was repeated until no crystallization during cooling was evident. The heat flow evolving during the isothermal crystallization was recorded as a function of time and the completion of the crystallization process was detected by the leveling of the DSC trace. For a better definition of the starting time (t_o), for each isothermal scan a blank runs were also performed with the same sample, at a temperature above the melting point where no phase change occurred [27]. The blank run was subtracted from the isothermal crystallization scan and the start of the process was taken as the intersection of the extrapolated baseline and the resulting exothermal curve.

Optical Crystallization Measurements

The isothermal rate of crystallization was also measured through the observation of the spherulitic radial growth, using an Olympus BH-2 optical microscope fitted with an Olympus DP/2 digital camera and a Linkam hot stage TP-93. Measurements were performed on a small fragment of polymer, inserted between two microscope cover glasses, and heated to 250°C for 3 min (where the melt was squeezed into a film through a small pressure applied to the upper glass), then quenched by means of

N_2 gas flow (cooling rate >250°C/min) to the selected crystallization temperature T_c, where isothermal crystallization was carried out. The complete crystallization process was recorded on a videotape and the diameter of the spherulites measured as a function of time, until impingement. Linear growth rates (G) were obtained from the average of the linear plots of the spherulite radius versus time. At least three spherulites per view area were measured for each crystallization temperature. Following this method G values were obtained with uncertainties of $\pm 0.01 \times 10^{-6}$ cm/s.

X-Ray Diffraction Measurements

The wide-angle x-ray diffraction measurements were performed on powdered crystallized samples at room temperature with a Rigaku Geiger Flex D-Max IIIa X-ray diffractometer, using Ni filtered Cu K_α radiation. The scanning rate was set at 5°/min, with the x-ray generator operated at 40 kV and 30 mA.

RESULTS AND DISCUSSIONS

Phase Behavior and Interchange Reactions

Before the discussion of crystallization kinetics, the phase behavior of the PTT/PC blends is discussed briefly. Figure 1 summarizes previous results on the thermal behavior of blends over the whole composition range [26]. The T_g's, of blends were obtained by DSC measurements at a heating of 20°C/min and by DRS at a heating rate of 1°C/min on melt-quenched samples. The amorphous characteristic of these samples were examined by wide-angle x-ray scattering measurements. The diffraction patterns were essentially featureless, suggesting the amorphous state. The crystallization temperature (T_c) and the melting temperature (T_m) correspond to the maximum of the exothermic and endothermic peaks observed in the DSC traces. As shown in Fig. 1, only one T_g is observed for all compositions. The value of T_g (DRS at 1 kHz) are slightly higher than the value of T_g (DSC), because of the higher frequency of DRS. In both cases, the T_g of the blends rises with increase of the PC content in the blend, suggesting miscibility of these melt-quenched blends, at least at the detection level of DSC (and DRS). The T_c values increased while the observed T_m values decreased with increasing PC composition. This behavior is usually observed in the case of miscible blends [28]. When the content of PC reach more than 40 wt % no cold crystallization peaks could be detected for the PTT component during the heating scan, indicating the inhibition of PTT crystallization in these high T_g'*s* blends.

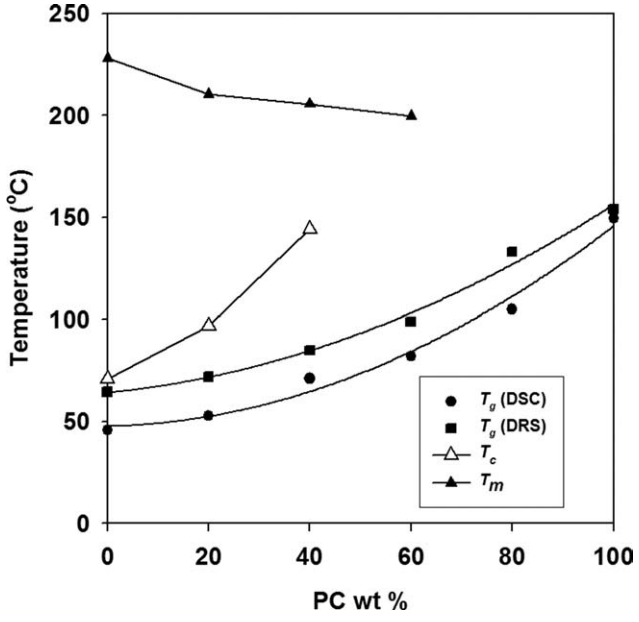

FIG. 1. Phase diagram of the PTT/PC blend samples after melt quenching, using data from Ref. 23. Lines are guides for eye.

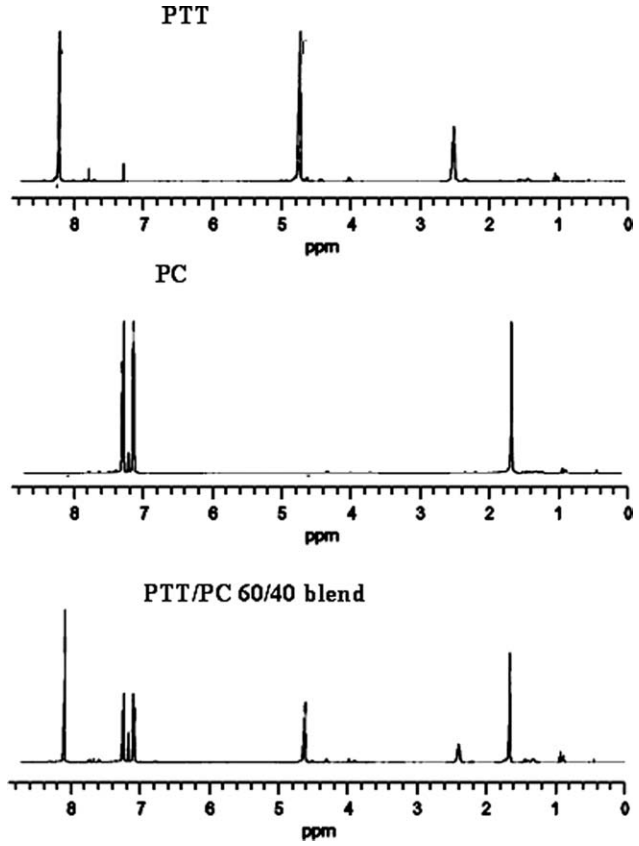

FIG. 2. ^{1}H NMR spectra of pure homopolymers and the PTT/PC 60/40 blend.

It is well known that transesterification in polyester blends can affect the crystallization behavior of PTT in the blends [29, 30]. The trans-reaction between PTT and PC in PTT/PC blend was analyzed by ^{1}H NMR spectra. Figure 2 shows the spectra of a representative PTT/PC 60/40 blend together with the neat polymers. The spectra

 DOI 10.1002/pen

of the blend show all the characteristic peaks of PTT and PC with no new peaks, indicating no detectable chemical changes occurred in the blends.

To check that trans-reaction did not affect the crystallization data, DSC studies were carried on the 60/40 PTT/PC blend. The sample was heated at a rate of 20°C/min from room temperature to 260°C, held at 260°C for several minutes, and subsequently cooled to room temperature at a rate of 10°C/min. The samples were then heated from 20 to 240°C at a rate 10°C/min to observe its melting behavior. This cycle was applied to the same sample for several times until transesterification was observed. Figure 3 illustrates the results of this experiment. It was found from the DSC heating curves that the melt annealing of the 60/40 PTT/PC blend at 260°C for 3, 6, and 9 min did not produce any significant changes in melting endothermic peak of PTT. In contrast, sample melt annealed at 260°C for 30 min shows a depression in the melting point as well as a reduction in the melting enthalpy of PTT. Eventually, at extended annealing times (1 h) the melting endothermic peak of PTT disappeared. This effect is better seen in Table 1, and is attributed to a higher extent of transesterification reaction between PTT and PC components during the extended annealing period. This series of experiments confirms the assumption that the crystallization data of a blend sample, held at 260°C for a period of time shorter than 5 min, are not influenced by transesterification.

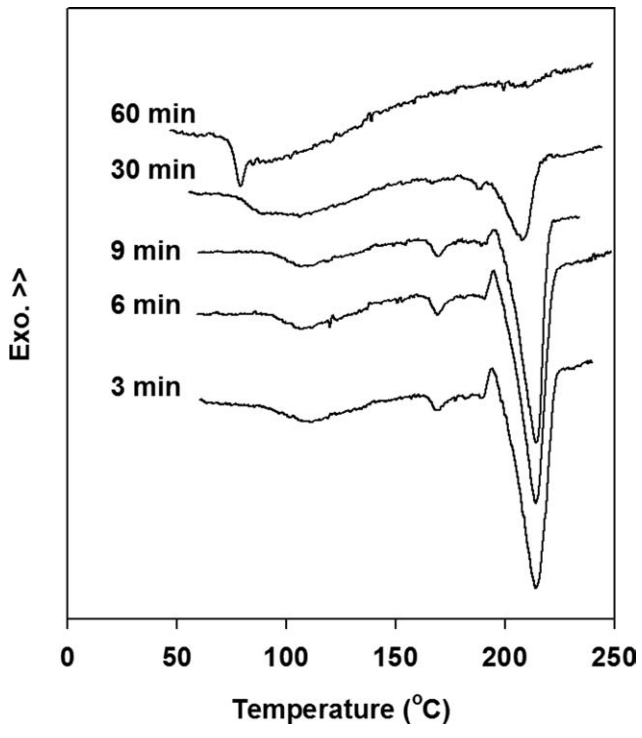

FIG. 3. DSC heating scan of the PTT/PC 60/40 blend samples melt annealed at 260°C for various time and subsequently cooled to room temperature.

TABLE 1. Melting temperature and enthalpy of fusion for the PTT/PC 60/40 blends after melt annealing at 260°C for various times, cooled to room temperature and subsequently heated to 240°C.

Melt annealing time (min)	T_m (°C)	ΔH_m (J/g)
3	214 ± 1	24
6	214 ± 1	23
9	215 ± 1	22
15	208 ± 1	10
60	210 ± 1	2

Isothermal Crystallization Kinetics

The analysis of isothermal bulk crystallization kinetics is often performed using the Avrami equation concerning phase transformation [31], which is usually written in the form:

$$X_t = 1 - \exp[-k_n(t - t_o)^n] \quad (1)$$

where X_t is the fraction of polymer crystallized at time t, k_n the overall kinetic constant, t is the time of the isothermal step measured from the achievement of the temperature control, t_o the initial time of the crystallization process, as described in the Experimental part, and n the Avrami exponent, which is correlated with the nucleation mechanism and the morphology of the growing crystallites. X_t can be calculated as the ratio between the area of the exothermic peak at time t and the total measured area of crystallization, assuming that the evolution of crystallinity is linearly proportional to the evolution of heat released during the course of crystallization. Figure 4a and b depict, as examples, the crystallization exotherms of neat PTT and PTT/PC blends at 190 and 205°C, respectively. It is observed that the crystallization exothermic peak shifted to larger time, and the width of peak increased with increasing PC composition. Figures 5a and b show the corresponding temporal development of $X(t)$ for various compositions at the same crystallization temperatures. As can be seen, all the curves have a sigmoidal shape, typical of polymer crystallization behavior. Furthermore, the initial slope of the isotherms decreased with increasing PC content, indicating progressively slower crystallization rate. This means that the presence of PC would strongly retard the overall crystallization kinetics of PTT.

It is likewise worth remembering that *Eq. 1* is usually applied to experimental data in the linearized form, by plotting $\ln(-\ln(1 - X_t))$ as a function of $\ln(t - t_o)$, permitting the determination of n and k_n from the slope and the intercept, respectively. In Fig. 6a and b, the linearized Avrami plots are shown for the selected set of crystallization temperatures. Similar plots were obtained for PPT and its blends at other T_c's. To evaluate k_n and n, only the experimental data at low conversion are used (i.e., data at high conversions are omitted from Fig. 6). The

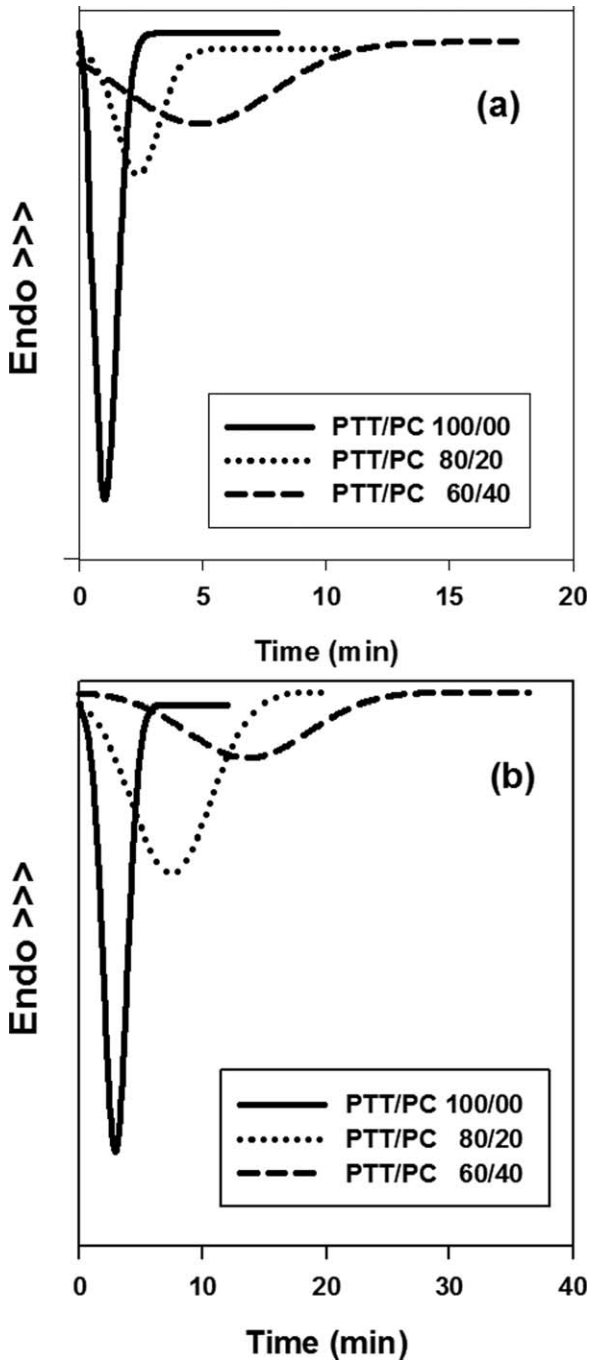

FIG. 4. DSC curves for the isothermal crystallization of the neat PTT and the PTT/PC blends at: (a) 190°C and (b) 205°C.

values of k_n and n determined by the intercepts and slopes, respectively, of these straight lines are listed in Table 2. To unify the units of the rate constant as min^{-1}, the rate constant was modified as $k_n = k^{1/n}$. Examining the data relative to each thermal treatment applied to the sample, one can observe that the overall kinetic constant k regularly decreases with increasing T_c, as usually happens at low undercooling, where crystal formation is controlled by nucleation. On the other hand, the values of k decrease with the addition of PC at the same crystallization temperature. The reason why the addition of PC reduces the crystallization rate may be related to the following three factors: (i) the addition of high T_g component (i.e. PC) increases the T_g of PTT/PC blends, resulting in the decrease of the mobility of blended PTT compared with that of neat PTT, (ii) the decrease of the melting point temperature of PTT in the blend may reduce the thermodynamic driving force required for the crystallization of PTT, and (iii) the added PC may have a diluent effect on the crystallization of PTT at the crystal growth front

The Avrami exponent n is close to three for all the crystallization temperatures and compositions investigated. This indicates that the nucleation mechanism and growth geometry of PTT crystals in blends were not

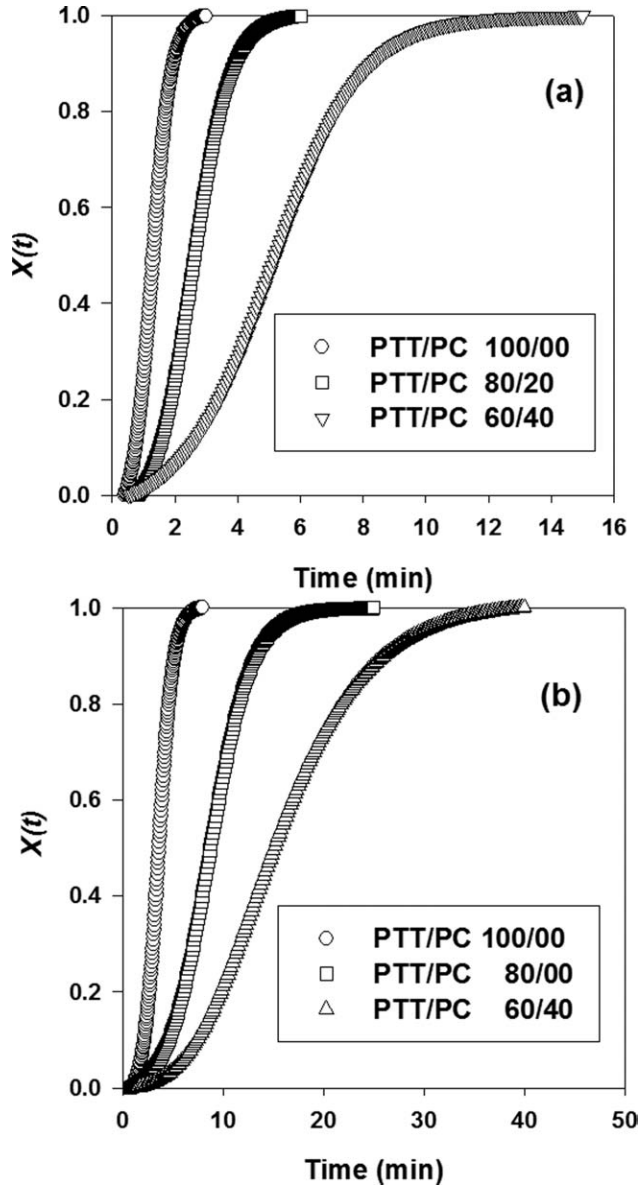

FIG. 5. Temporal evolution of relative crystallinity as a function of crystallization time for the neat PTT and the PTT/PC blends at: (a) 190°C and (b) 205°C.

DOI 10.1002/pen

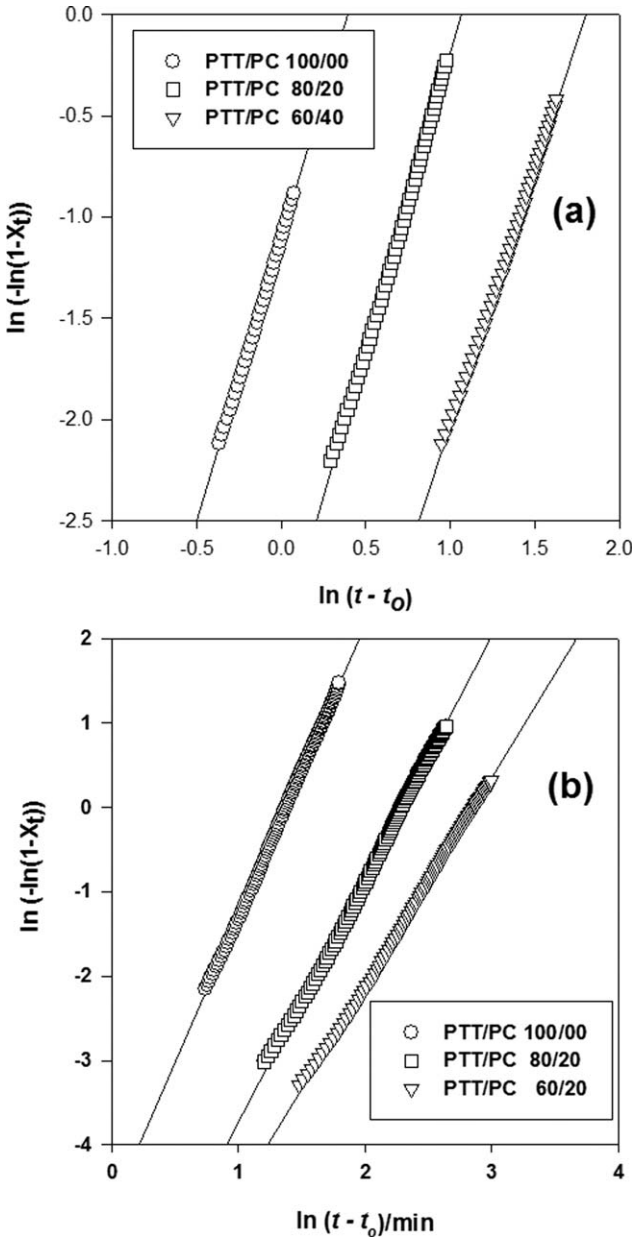

FIG. 6. Linearized Avrami plots for the neat PTT and the PTT/PC blends at: (a) 190°C and (b) 205°C.

affected by the presence of PC and the crystallization process originates from predetermined nuclei and is characterized by three-dimensional spherulitic growth.

The half-time of crystallization, $t_{0.5}$, defined as the time required to attain half of the final crystallinity is an important parameter for the discussion of crystallization kinetics. Its value can be obtained from the following relationship:

$$t_{0.5} = \left(\frac{\ln 2}{k_n}\right)^{1/n} \tag{2}$$

where k_n and n are the same as in the Avrami equation. Usually, the crystallization rate can also be described as

TABLE 2. Avrami kinetic parameters for the isothermal crystallization of PTT/PC blends.

Blend composition	T_c (°C)	$t_{0.5}$ (min)	$n \pm 0.2$	k (min^{-1}) $\times 10^{-4}$
PTT/PC (100/00)	190	1.0	2.8	6.8
	195	1.3	3.0	5.3
	200	2.0	3.1	3.4
	205	2.7	2.9	2.6
PTT/PC (80/20)	190	2.5	2.9	2.7
	195	3.2	2.9	2.1
	200	4.9	2.9	1.4
	205	6.7	2.6	1.0
PTT/PC (60/40)	190	4.2	2.5	1.7
	195	5.9	2.8	1.2
	200	9.1	2.8	0.76
	205	12.3	2.4	0.57

the reciprocal of $t_{0.5}$, i.e., $1/t_{0.5}$. Figure 7 shows the variation of $1/t_{0.5}$ as a function of crystallization temperature and blend composition. The value of $1/t_{0.5}$ decreases with increasing crystallization temperature as well as the addition of PC, indicative of the reduction of crystallization rate. These results are consistent with the trend of the rate constant k listed in Table 1. All the aforementioned results can lead us to a conclusion that the addition of PC does not change the overall crystallization mechanism of PTT, but only reduces the crystallization rate in the PTT/PC blends.

Morphology and X-Ray Differaction

The size and the average size distribution of PTT crystals, as well as, their shape and orientation determine the

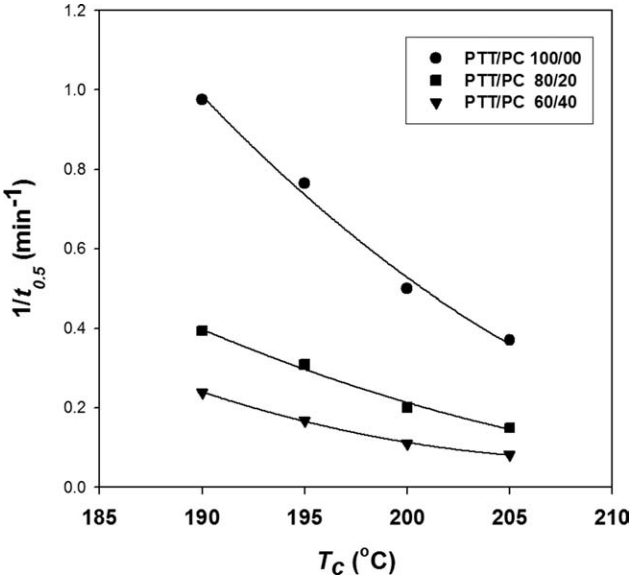

FIG. 7. Half-times of crystallization for neat PTT and its blends with PC at various crystallization temperatures.

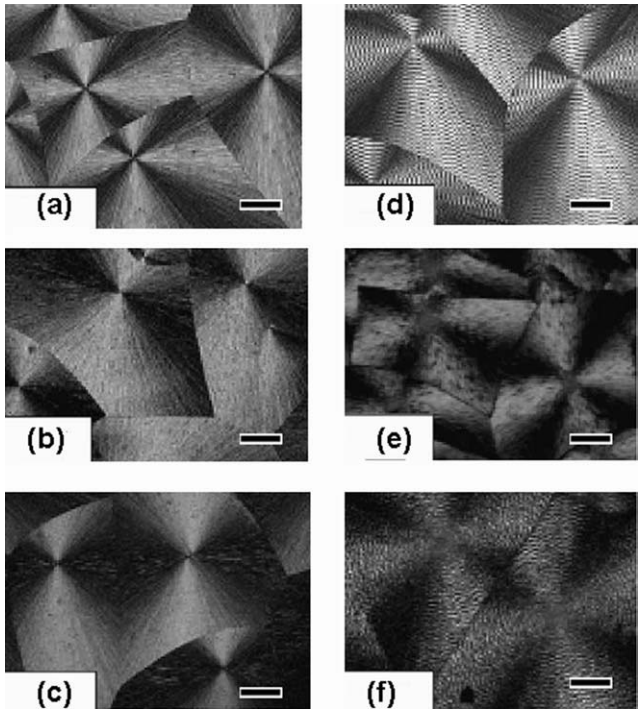

FIG. 8. POM micrographs (A ⊥ B) of the spherulite morphology of (a) neat PTT, (b) PTT/PC 80/20 blend, (c) PTT/PC 60/40 blend at T_c of 190°C and (d), (e), (f) at T_c of 205°C, respectively. Scale bar = 40 mm.

melt behavior of the material and depend exclusively on the conditions of nucleation and growth of crystals. The size of spherulites depends on the ratio between the nucleation rate and the growth rate of crystals, thus the kinetics of crystallization determines the morphology and the degree of crystallinity of the polymer. Polarized optical micrographs (POM's) showing the superstructure of pure PTT and PTT/PC blends, submitted to isothermal crystallization at 190 and 200°C, respectively, are shown in Fig. 8. It can be seen that pure PTT displays a spherulitic form that exhibit concentric extinction bands. The texture of PTT spherulites becomes more open with increasing PC content in the blends (see Fig. 8). In addition, the band spacing becomes larger with increasing the noncrystallizable component concentration. The number of spherulites in the PTT crystallized at 190°C is higher than that crystallized at 200°C (see Fig. 8). It means that the nucleation rate is higher than growth rate at 190°C. The micrographs show a volume completely filled with the spherulites and no PC phase was observed among the spherulites. These observations and the fact that the PC influences the crystallization kinetics and morphology of crystalline PTT suggest that the noncrystallized component is segregated in the interlamellar regions. That is PC molecules diffuse away from the front of PTT crystallization at a rate not sufficient to let them move away from the spherulites.

To check that PC did not co-crystallize with PTT by being incorporated into the crystalline regions, wide angle X-ray diffraction studies were carried out on the crystalline blends. The diffraction patterns of the blends were similar to that obtained from PTT. Figure 9 shows the WAXD patterns of neat PTT and the PTT/PC (80/20) blend isothermally crystallized at 205°C. There were no additional peaks present and the reflection positions are not affected by the addition of PC, indicating that the unit-cell parameters remain unchanged. However, the intensity of these characteristic peaks slightly decreases with the presence of PC, implying an overall reduction in blend crystallinity and that the crystalline phase was PTT only.

Spherulitic Growth Kinetics

For further investigation, the study of the transient growth of polymer spherulites can also provides more fundamental aspects of the crystallization process at the microscopic level. The isothermal transient development of the spherulites of the neat PTT and its blends with PC were monitored microscopically at various T_c's, in the range of 185–205°C. For the neat PTT the radius of spherulites (R) increased linearly with time up to the point of impingement with adjacent spherulites. Similar results are obtained for all the blends except that the spherulitic texture, as can be seen in Fig. 8c, became coarser with more open texture and less well-defined boundaries between the spherulites and the melt with increasing PC content. This is consistent with crystallization of the PTT as spherulites and rejection of the PC into the interlamellar region. The spherulitic growth rate (G) for a given

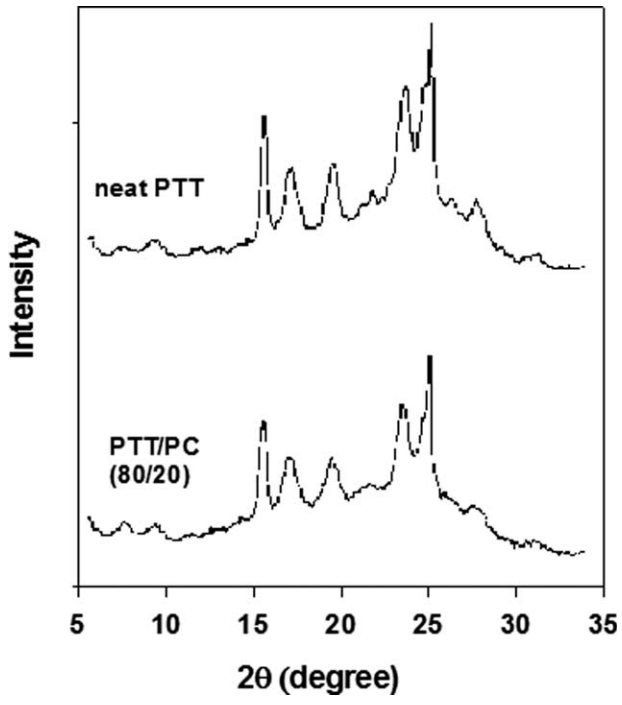

FIG. 9. WAXD profiles of the neat PTT and the PTT/PC 80/20 blend isothermally crystallized at 205°C for 1 h.

DOI 10.1002/pen

sample type and T_c was calculated from the slope of a least-squared line drawn through the obtained $R(t)$ function. Figure 10 shows the measured growth rates for the neat PTT and PTT/PC blends at different T_c's. Within the T_c range investigated, plots of G as a function of T_c, for a given sample type, showed a monotonic decrease in the G values with increasing T_c. The spherulite growth rate of PTT decreases dramatically as the crystallization temperature is increased whereas for the blends the spherulite growth rate becomes very slow over the whole range of crystallization temperatures measured.

The spherulite growth rates can be treated according to the secondary nucleation theory of Lauritzen and Hoffman [32]. According to this theory the dependence of the growth rate G on the crystallization temperature T_c and on the undercooling $\Delta T = T_m^o - T_c$, is described by the following equation:

$$G = G_o \exp[-U^*/R(T_c - T_\infty)] \exp[-K_g/T_c \Delta T f] \quad (3)$$

where G_o is a pre-exponential factor assumed to be independent of temperature and U^* is the activation energy for the transport of polymer segments across the liquid/crystal interface, T_∞ is the temperature at which the transport of segments across the liquid-solid interface becomes infinitely slow and is defined as $T_\infty = T_g - C$, where C is a constant; R is the gas constant; and f is a correction factor accounting for the change of melting enthalpy with temperature and is given by $2T_c/(T_m^o - T_c$; where T_m^o is the equilibrium melting temperature. K_g is the nucleation constant, expressed as:

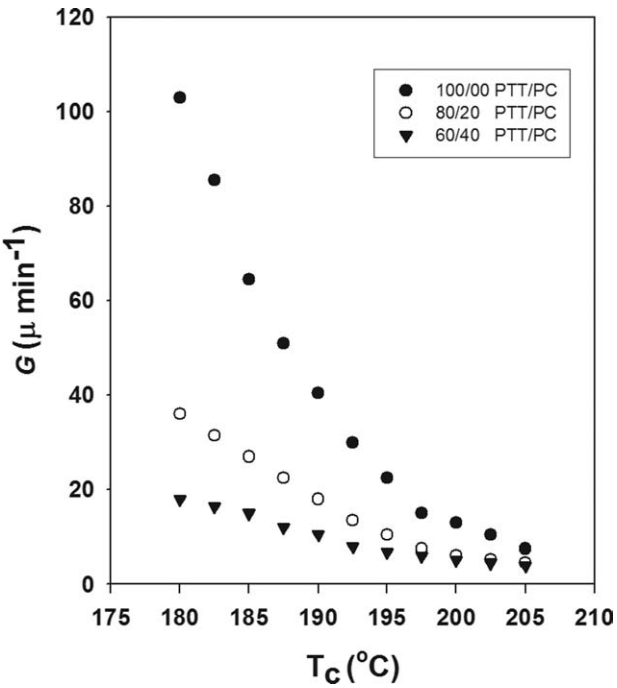

FIG. 10. The spherulitic growth rates for the neat PTT and PTT/PC blends at different crystallization temperatures.

$$K_g = n_e b_o \sigma \sigma_e T_m^o / \Delta H_m^o k \quad (4)$$

where n_e is a constant representing the regime of crystallization ($n_e = 4$ for regime I and III and $n_e = 2$ for regime II), σ and σ_e are the surface free energies per unit area of the crystalline lamellae that run parallel and perpendicular to the chain direction, respectively, k is Boltzmann's constant, b_o is the distance between two adjacent fold planes which in the case of PTT is taken as $d_{010} = 5.71 \times 10^{10}$ m [33]. This value corresponds to the perpendicular separation of crystal growth planes, which is not equal to the b parameter of the crystal unit cell; the latter being triclinic for PPT [33]. ΔH_m^o is the equilibrium melting enthalpy and was estimated to be 2.073×10^9 J/m^3 [34]. For a polymer-diluents system, *Eq. 3* was modified by Boon and Azcue [35]:

$$\ln G - \ln \phi + \frac{U^*}{R(T_c - T_\infty)} - \frac{0.2 T_m^o \phi_2}{\Delta T} = F(G) = \ln G_o - \frac{K_g}{T_c(\Delta T) f} \quad (5)$$

In this equation, the pre-exponential factor is multiplied by the PTT volume fraction ϕ_2 because the rate of nucleation is proportional to the concentration of crystallizable units.

When isothermal crystallization is studied far above the T_g, the exact values of U^* and T_∞ hardly affect the temperature dependence of the rate constant (nucleation control vs. transport control), and standard values are usually employed. The most commonly used are the Williams-Landel-Ferry [36] values ($U^* = 4120$ cal/mol and $T_\infty = T_g - 51.6K$) and those reported by Suzuki and Kovacs [37] ($U^* = 1500$ cal/mol and $T_\infty = T_g - 30K$). In fact this value greatly affects the application of the HF theory in qualitative and quantitative estimations, because a modification of this parameter would lead to a significant change in the apparent temperature of regime transition [38]. In the calculation, we didn't use for U^* the standard values, usually employed for most polymers: $U^* = 2500$ cal/mol was chosen, as suggested by Hong et al. [33]. These authors obtained this value by means of a common simulation method [38–40] applied to their crystallization data. Their simulation results shows that at the lower T_c, the data diverge upwards and downwards with changing U^* value. Meanwhile, the U^* value of 2500 cal mol^{-1} could be determined to permit the best linear fit of the data, indicating that this value is relatively suitable for use in PTT.

The nucleation factor K_n, as defined in *Eq. 4*, represents the energy to form a nucleus of critical size. Its value is determined by plotting the left-hand side of *Eq. 5* versus $1/T_c(\Delta T)f$ (thereafter the H-F plot). Figure 11 present the H-F plots for PTT and PTT/PC blends; in these calculations the value of $T_m^o = 525$ K of neat PTT [34] was used through all data, neglecting the depression in

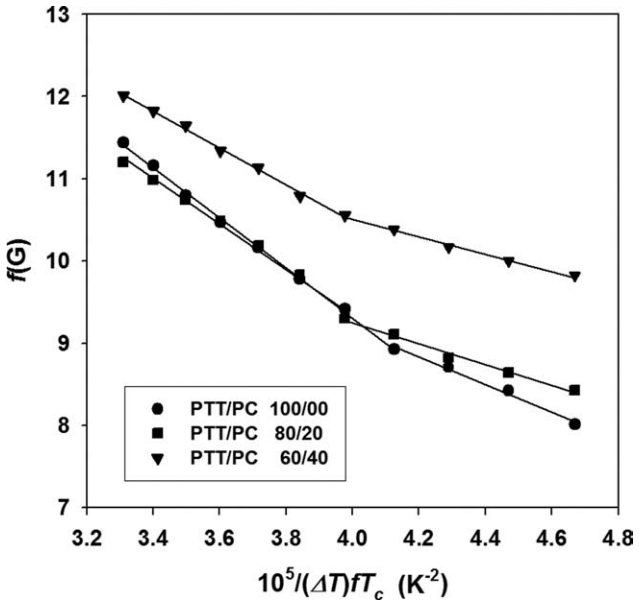

FIG. 11. Lauritzen-Hoffman kinetic plots for the isothermal crystallization of the neat PTT and the PTT/PC blends. The line represent the fit to *Eq. 5* (see the text).

T_m^o of the blends. According to *Eq. 5*, regime I→II transition is evident when a downward change in slope is observed, whereas, for regime II→III, an upward change in slope is expected [32]. Figure 11 clearly indicates that neat PTT and the blends exhibit the classical regime II→III transition. The transition occurred at around 198°C for the neat PTT, which is slightly higher than that observed by Hong et al. [33], being 195°C.

Interestingly, the blends exhibited a lower regime II→III transition temperature; it is 194°C for the 60/40 PTT/PC blend. A reduction of temperature of the regime II-III transition with composition has been reported for several polymer pairs, such as P(3-HB)/PVAc [41] and PCL/PH [42]. Since the rate of secondary nucleation is much higher in regime III than in regime II. The presence of the diluent may causes a diminution in the rate of secondary nucleation. That is, at parity of temperature, in the plain homopolymer solidification can occur according to regime III, and the addition of the amorphous component may favor regime II growth.

The K_n values determined from the slops of the H-F lines are given in Table 3. The ratio of $K_{g(III)}$ to $K_{g(II)}$ for neat PTT and the blends was close to 2.0, as expected according to the secondary nucleation theory [32]. Figure 12 shows Temperature dependence of the crystal growth rate for regime III (solid line) and regime II (dashed line). These curves were calculated by *Eq. 5*, giving the estimated U^* and T_∞ parameters, and the deduced values of ln G_o and K_g for each regime. The calculated curves fit well with the experimental spherulitic growth data.

The derived K_g's can be used to calculate the product of the surface free energies, $\sigma\sigma_e$ and the fold-surface free energy σ_e. An estimation of σ can be obtained by the following empirical equation [43]:

$$\sigma = \alpha \Delta H_m^o \sqrt{a_o b_o} \tag{6}$$

where $a_o b_o$ is the cross-sectional area of the polymer and α is the Thomas-Stavely empirical parameter, with value ranging between 0.1 and 0.3. The α value is not at all universal and strongly depends on the chemical structure of the polymer, and it is related to entropy differences between the crystal and the melt interface. Generally, α is usually assumed to be 0.1 for polyolefins and 0.25 for polyesters [43]. From a characteristic ratio (C_∞) describing the unperturbed dimension of a polymer chain and the mean-square end-to-end distance $<r^2>$ of a long polymer chain in the unperturbed state, Hong et al. [33] evaluate the value of α as 0.18. In this work, α is chosen to be 0.18. The lateral surface free energy of PTT turned out to be 19.2 erg/cm^2. By combination of *Eqs. 4* and *6* the values of the fold-surface free energy σ_e for neat PTT and the blends were derived and are listed in Table 3. A decrease of σ_e with increase of the content of PC has been found. A similar trend has been reported for a series of polymer blends [44–47]. This decrease has been explained supposing that the presence of the amorphous component, influencing the crystallization process, produces an increase of the folding entropy and relates to the formation of crystals with more disordered folding surfaces. It must be noted that, in all the literature examples, the melt viscosity increases with the increase of amorphous material content; as in the PTT/PC system under this investigation.

An additional quantity of interest, namely the work of chain folding (q) [32] can be calculated from the following:

$$q = 2\sigma_e a_o b_o \tag{7}$$

It has to be emphasized that q is a parameter closely correlated with the molecular structure, i.e., the inherent

TABLE 3. Results of the secondary nucleation analysis for neat the PTT and the PTT/PC blends.

PTT/PC	ln $G_{o\ (III)}$	$K_{g\ (III)} \times 10^5$ (K^2)	$\sigma_{e\ (III)}$ (erg/cm^2)	$q_{\ (III)}$ (kcal/mol)	r^2	ln $G_{o\ (II)}$	$K_{g\ (II)} \times 10^5$ (K^2)	$\sigma_{e\ (II)}$ (erg/cm^2)	$q_{\ (II)}$ (kcal/mol)	r^2	$T_{II\to III}$ (°C)
100/00	21.5	3.04 ± 0.1	53.2	4.1	0.9986	15.88	1.68 ± 0.1	58.8	4.5	0.9894	198
80/20	20.4	2.77 ± 0.1	48.5	3.7	0.9916	14.33	1.27 ± 0.1	44.5	3.4	0.9909	195
60/40	19.5	2.24 ± 0.1	39.2	3.0	0.9967	14.77	1.06 ± 0.1	37.1	2.8	0.9930	194

 DOI 10.1002/pen

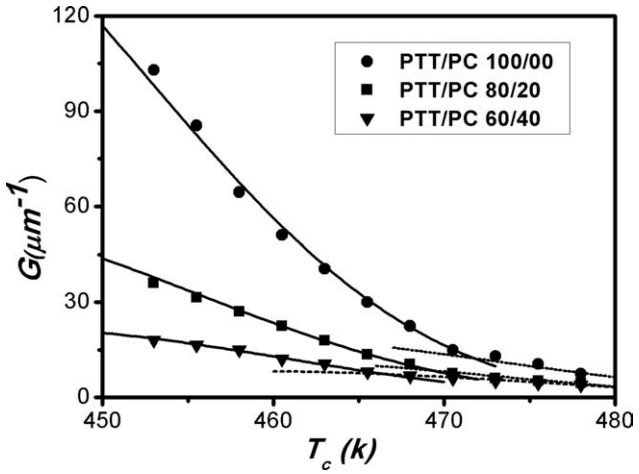

FIG. 12. Temperature dependence of the crystal growth rate according to *Eq. 5* for regime III and regime II using fit parameters listed in the text. Experimental growth rates are also shown as symbols for comparison.

stiffness of the chain itself. The values of q for various samples are listed in Table 3. The q values for the neat PTT and its blends with PC were found to be in the range of 4.5 and 2.8 kcal mol^{-1}, with the values for the blends smaller than that of the neat PTT.

CONCLUSION

The Avrami and L-H secondary nucleation theories were applied to analyze the crystallization and the spherulitic growth kinetics of neat PTT and its blends with PC. Blending with PC did not change the crystallization mechanism of PTT, but reduced the crystallization rate compared with that of neat PTT at the same crystallization temperature. The spherulitic morphologies of the PTT blends showed linear impingement between the spherulites, indicating that PC was predominantly segregated into PTT interlamellar and/or interfibrillar regions after PTT crystallization. This observation was consistent with the average value of 2.9 for the Avrami exponent, which indicated three-dimensional growth of crystals following an athermal nucleation event. The spherulitic growth rate of PTT decreased upon blending. Through the L-H analysis a transition from regime II to regime III around 197°C was observed for pure PTT. The temperature of the regime transition decreased in the blends. The L-H parameters of neat and blended PTT were derived and compared with each other including the nucleation parameter (K_g), the fold-surface free energy (σ_e), and the work of chain folding (q). Blending with PC decreased all the aforementioned parameters compared with those of neat PTT.

ACKNOWLEDGMENTS

El Shafee acknowledges a visiting scholarship received from the CAS-TWAS Program.

REFERENCES

1. D.R. Paul and S. Newman, *Polymer Blends*, Vols. **I** and **II**, Academic, London (1978).
2. L.A. Utracki, *Polymer Blends and Alloys: Thermodynamics and Rheology*, Hanser, Munich (1989).
3. J. Grebowicz and H.H. Chauh, *Progress Report*, Shell Chemical Co. Houston, Texas, USA (1996).
4. K. Dangayach, H.H. Chuah, W. Gergen, P. Dalton, and F. Smith, "Plastic—Saving Planet Earth," *Proceedings of 55th ANTEC Conference*, Toronto, 2097 (1997).
5. W.B. Liau, A.S. Liu, and W.Y. Chiu, *J. Polym. Res.*, **6**, 27 (1999).
6. F.G. Chiu, K.H. Huang, and J.C. Yang, *J. Polym. Sci. Phys.: Part B, Polym. Phys.*, **41**, 2264 (2003).
7. J. Ramiro, J.I. Eguiazabal, and J. Nazabal, *Polym. Adv. Techon.*, **14**, 129 (2003).
8. P. Supaphol, N. Dangseeyun, P. Thanomkiat, and M Mithitanakul, *J. Polym. Sci.: Part B Polym. Phys.*, **42**, 676 (2004).
9. M. Castellano, A. Turturro, B. Valenti, A. Avagliano, and G. Costa, *Mocromol. Chem. Phys.*, **207**, 242 (2006).
10. D.H. Huang, E.M. Woo, and L. Lee, *Colloid Polym. Sci.*, **284**, 843 (2006).
11. I. Gonzalez, I. Eguiazabal, and J. Nazabal, *J. Appl. Polym. Sci.*, **102**, 3246 (2006).
12. W.J. Bae and W.H. Jo, *Macrmol. Res.*, **10(3)**, 145 (2002).
13. A. Yavari, A. Asadinezhad, S.H. Jafari, H.A. Khonakdar, F. Boehme, and R. Haessler, *Eur. Polym. J.*, **41**, 2880 (2005).
14. M.L. Xue, J. Sheng, H.H. Chuah, and X.Y. Zhang, *J. Macromol. Sci. Phys. B*, **43**, 1045 (2004).
15. M.L. Xue, Y.L. Yu, J. Sheng, H.H. Chuah, C.H. Geng, *J. Macromol. Sci. Phys. B*, **44**, 317 (2005).
16. F. C. Chiu and M.H. Ting, *Polym. Test*, **26**, 338 (2007).
17. L.T. Lee and E.M. Woo, *Colloid Polym. Sci.*, **282**, 1308 (2004).
18. S.K. Na, B.G. Kong, C.Y. Choi, M.K. Jang, J.W. Nah, H.G. Kim, and B.W. Jo, *Macromol. Res.*, **13**, 88 (2005).
19. S.J. Oh, D.W. Chae, H.J. Lee, and B.C. Kim, *Polym. Mat. Sci. Eng.*, **84**, 621 (2001).
20. M.L. Xue, Y.L. Yu, J. Sheng, and H.H. Chuah, *J. Macromol. Sci. Phys. B*, **44**, 531 (2005).
21. W.J. Bae, W.H. Jo, and M.S. Lee, *Polym. Mat. Sci. Eng.*, **84**, 668 (2001).
22. W.J. Bae, W.H. Jo, and K.M. Park, *Macromol. Res.*, **10**, 145 (2002).
23. M. Guo and W.J. Brittain, *Macromolecules*, **31**, 7166 (1998).
24. Y.H. Kuo and E.M. Woo, *J. Polym. Sci. Polym. Phys. Ed.*, **41**, 2394 (2003).
25. Y. Takoda and D.R. Paul, *Polymer*, **33**, 3389 (1992).
26. E. El. Shafee, G.R. Saad, and M. Zaki, *J. Polym. Res.*, **15**, 47 (2008).
27. M.C. Righetti and A. Munari, *Macromol. Chem. Phys.*, **198**, 363 (1997).
28. J.M. Huang and F.C. Chang, *J. Appl. Polym. Sci.*, **84**, 850 (2002).
29. J. Devaux, P. Godard, and J.P. Mercier, *Polym. Sci. Part B: Polym. Phys.*, **20**, 1875 (1982).

30. M. Kimura and J.P. Porter, *J. Polym. Sci. Part B: Polym. Phys*, **21**, 367 (1983).
31. M. Avrami, *J. Chem. Phys*., **9**, 177 (1941).
32. J.D. Hoffman, G.T. Davis, and J.I. Lauritzen Jr., "*Treatise on Solid State Chemistry*," 1st ed., N.B. Hannay, Ed., Vol. 3, Chapter 7, Plenum Press, New York (1976).
33. P.D. Hong, W.T. Chung, and C.F. Hsu, *Polymer*, **43**, 3335 (2002).
34. W.T. Chung, W.J. Yeh, and P.D. Hong, *J. Appl. Polym. Sci*., **83**, 2426 (2002).
35. J. Boon and J.M. Azcue, *J. Polym. Sci. Part A: Polym. Chem*., **6**, 885 (1968).
36. M.L. Williams, R.F. Landel, and J.D. Ferry, *J. Am. Chem. Soc*., **77**, 3701 (1955).
37. T. Suzuki and A.J. Kovacs, *Polym. J*., **1**, 82 (1970).
38. F.J. Medellin-Robrigues, P.J. Philips, and L.S. Lin, *Macromolecular*, **28**, 7744 (1995).
39. A.J. Lovinger, D.D. Davis, F.J. Padden Jr., *Polymer*, **26**, 1595 (1085).
40. L.H. Palys and P.J. Philips, *J. Polym. Sci. Part B: Polym. Phys*., **18**, 829 (1980).
41. P. Greco and E. Martuscelli, *Polymer*, **30**, 1475 (1989).
42. R. de Juana and M. Cortazar, *Macromolecules*, **26**, 1170 (1993).
43. J.I. Lauritzen Jr. and J.D. Hoffman, *J. Appl. Phys*., **44**, 4340 (1973).
44. S. Cimmino, E. Martuscelli, C. Silvestre, M. Canetti, C. De Lalla, and A. Seves, *J. Polym. Sci. Part B: Polym. Phys*., **27**, 1781 (1989).
45. E. Dubini Paglia, P.L. Beltrame, M. Canetti, and A. Seves, *Polymer*, **34**, 996 (1993).
46. L.L. Zhang, S.H. Goh, S.Y. Lee, and G.R. Hee, *Polymer*, **41**, 1429 (2000).
47. E. Martuscelli, C. Silvestre, and C. Gismondi, *Makromol Chem*., **186**, 2161 (1985).

 DOI 10.1002/pen